FLORE
Repository istituzionale dell'Università degli Studi di Firenze

The Ethiopian subcontinental mantle domains: geochemical evidence from Cenozoic mafic lavas

Questa è la Versione finale referata (Post print/Accepted manuscript) della seguente pubblicazione:

Original Citation:

The Ethiopian subcontinental mantle domains: geochemical evidence from Cenozoic mafic lavas / S. TOMMASINI; P. MANETTI; F. INNOCENTI; T. ABEBE; M.F. SINTONI; S. CONTICELLI. - In: MINERALOGY AND PETROLOGY. - ISSN 0930-0708. - STAMPA. - 84:(2005), pp. 259-281. [10.1007/s00710-005-0081-9]

Availability:

The webpage https://hdl.handle.net/2158/308183 of the repository was last updated on

Published version:

DOI: 10.1007/s00710-005-0081-9

Terms of use:

Open Access

La pubblicazione è resa disponibile sotto le norme e i termini della licenza di deposito, secondo quanto stabilito dalla Policy per l'accesso aperto dell'Università degli Studi di Firenze (https://www.sba.unifi.it/upload/policy-oa-2016-1.pdf)

Publisher copyright claim:

La data sopra indicata si riferisce all'ultimo aggiornamento della scheda del Repository FloRe - The above-mentioned date refers to the last update of the record in the Institutional Repository FloRe

(Article begins on next page)

24 July 2025

Mineralogy and Petrology (2005) 84: 259–281
DOI 10.1007/s00710-005-0081-9

Mineralogy and Petrology

© Springer-Verlag 2005
Printed in Austria

The Ethiopian subcontinental mantle domains: geochemical evidence from Cenozoic mafic lavas*

S. Tommasini[1,3], **P. Manetti**[1,3], **F. Innocenti**[2], **T. Abebe**[1], **M. F. Sintoni**[1], and **S. Conticelli**[1,3]

[1] Dipartimento di Scienze della Terra, Università degli Studi di Firenze, Firenze, Italy
[2] Dipartimento di Scienze della Terra, Università degli Studi di Pisa, Pisa, Italy
[3] Istituto di Geoscienze e Georisorse CNR, Pisa, Italy

Received May 10, 2004; revised version accepted February 28, 2005
Editorial handling: P. Garofalo

Summary

Since the Cenozoic, Ethiopia was affected by a widespread volcanic activity related to the geodynamic evolution of the Afar triple junction. The plateau building phase was followed by the formation of the Main Ethiopian Rift (MER) accompanied by a bimodal volcanic activity in both the inner parts of the rift and its shoulders. Outside the rift, a concurrent volcanic activity occurred mainly along transversal tectonic lineaments, the most important of which is the Yerer-Tullu Wellel Volcano-Tectonic Lineament (YTVL) developing for ~500 km westward of Addis Abeba. Scattered Pliocene – Quaternary volcanoes are reported also inside the plateau such as those outcropping nearby Lake Tana.

Here we present the result of a study on carefully screened mafic lavas outcropping in two sectors located off-axis the MER, namely, the YTVL and the southern part of Lake Tana; and in one sector located in the southern tip of the MER close to Megado, in the Sidamo region. The screened samples are petrographically fresh and have $SiO_2 < 52$ wt.% and $MgO > 4$ wt.%, to minimise crystal fractionation effects. Most of the samples belong to the Late Miocene – Quaternary volcanic activity of the East African Rift System (EARS), although a number of samples along the YTVL are representative of the Late Eocene – Early Miocene Ethiopian Volcanic Plateau flood basalts. The selected mafic lavas offer the opportunity to assess the geochemical diversity, if any,

* Supplementary material to this paper is available in electronic form at http://dx.doi.org/10.1007/s00710-005-0081-9

of the subcontinental mantle domains along the MER (Megado and the easternmost part of the YTVL) and in sectors far away from the MER (YTVL and Lake Tana). The samples have a wide compositional range: from basanite to alkali basalt, hy-normative basalt, qz-normative basalt, basaltic andesite, hawaiite, trachybasalt, and trachyandesite. The major and trace element characteristics of the mafic lavas demonstrate an origin from a relatively fertile and trace element enriched lithospheric mantle at pressure variable from ~2.0 to 3.5 GPa. Moreover, systematic variations in K/Nb, Ba/Nb, and Ba/Rb demand for the contribution of trace amounts of phlogopite to melt production.

The geochemical signature coupled with the geographical distribution of the Late Miocene – Quaternary samples along the YTVL (~500 km) and the Lake Tana and Megado sectors set constraints on a relatively homogenous lateral continuity of the deeper lithospheric mantle domains (~2–3.5 GPa). On the other hand, the trace element characteristics of the Ethiopian Volcanic Plateau samples along the YTVL, demand for a chromatographic process *en route* to the surface and indicate a shallower lithospheric mantle domain (< 2 GPa) with a different geochemical signature. Overall, the selected mafic lavas provide evidence for vertically zoned lithospheric mantle domains: the shallower domain (< 2 GPa) consists of an enriched mantle component with a geochemical signature similar to continental crust material (EM II), whilst the deeper domain (~2–3.5 GPa) consists of an enriched component similar to the average composition of the subcontinental lithospheric mantle (SCLM).

Introduction

The geochemistry of mafic, alkaline volcanic rocks erupted in continental areas are unique benchmarks to assess the extent of the geochemical diversity and time-integrated heterogeneity of the subcontinental mantle. Geochemical and isotopic characteristics of basalts produced in continental areas are often anomalous compared to those of MORBs and OIBs of ocean basins (e.g., *Wilson*, 2000), and suggest the involvement of distinct sources, possibly including the lithospheric mantle. Melt production from the lithospheric mantle, however, is paradoxical because it is much colder than the convecting asthenosphere to account for its higher rigidity and attachment to continental plates, and it should be highly depleted in those major elements necessary for basalt generation (e.g., *Arndt* and *Christensen*, 1992). Enrichment processes involving percolation of silicate melts and volatile-rich fluids have been proposed to explain melt production at temperatures well below the solidus of dry peridotite (e.g., *Hawkesworth* et al., 1984; *Menzies* and *Hawkesworth*, 1987; *Stolz* and *Davies*, 1988). Other factors including extension rate, convection at various scales, lateral temperature gradients, and other inputs of external heat (i.e. mantle plumes) also may contribute (e.g., *McKenzie* and *Bickle*, 1988). The heterogeneity of the lithospheric mantle, as testified by the ubiquitous occurrence of metasomatised mantle xenoliths, is thus a product of interaction between cold stable lithosphere and the silicate melts or volatile-bearing fluids associated with asthenospheric magmatism (*Andersen* et al., 1984; *Jagoutz* et al., 1980; *Menzies* et al., 1985; *Gamble* et al., 1988; *Menzies* and *Halliday*, 1988; *Waters* and *Erlank*, 1988; *McDonough*, 1990).

The Afar triple junction, which includes the East African Rift System (EARS) and the Red Sea and Gulf of Aden rifts, is excellent for studying basalt composition as a function of mantle source heterogeneity and degree of melting, and in the last

decades a number of models have been proposed to account for its geodynamic evolution (e.g., *Baker* et al., 1972; *Berhe* et al., 1987; *Hart* et al., 1989; *Kampunzu* and *Mohr*, 1991; *Schilling* et al., 1992; *Deniel* et al., 1994; *George* and *Rogers*, 1999; *Rogers* et al., 2000; *Debayle* et al., 2001). In this paper we present the result of a study on the geochemical characteristics of mafic lavas outcropping in one sector located in the southern part of the Main Ethiopian Rift (MER) close to Megado, in the Sidamo region, and in two sectors located off-axis the MER, namely, the Yerer-Tullu Wellel Volcano-Tectonic Lineament (YTVL), central Ethiopia, and the southern part of Lake Tana, North Ethiopia (Fig. 1). The rationale of the selected sample localities is meant at tackling the diversity, if any, of the subcontinental mantle reservoirs underneath the Main Ethiopian Rift (Megado and

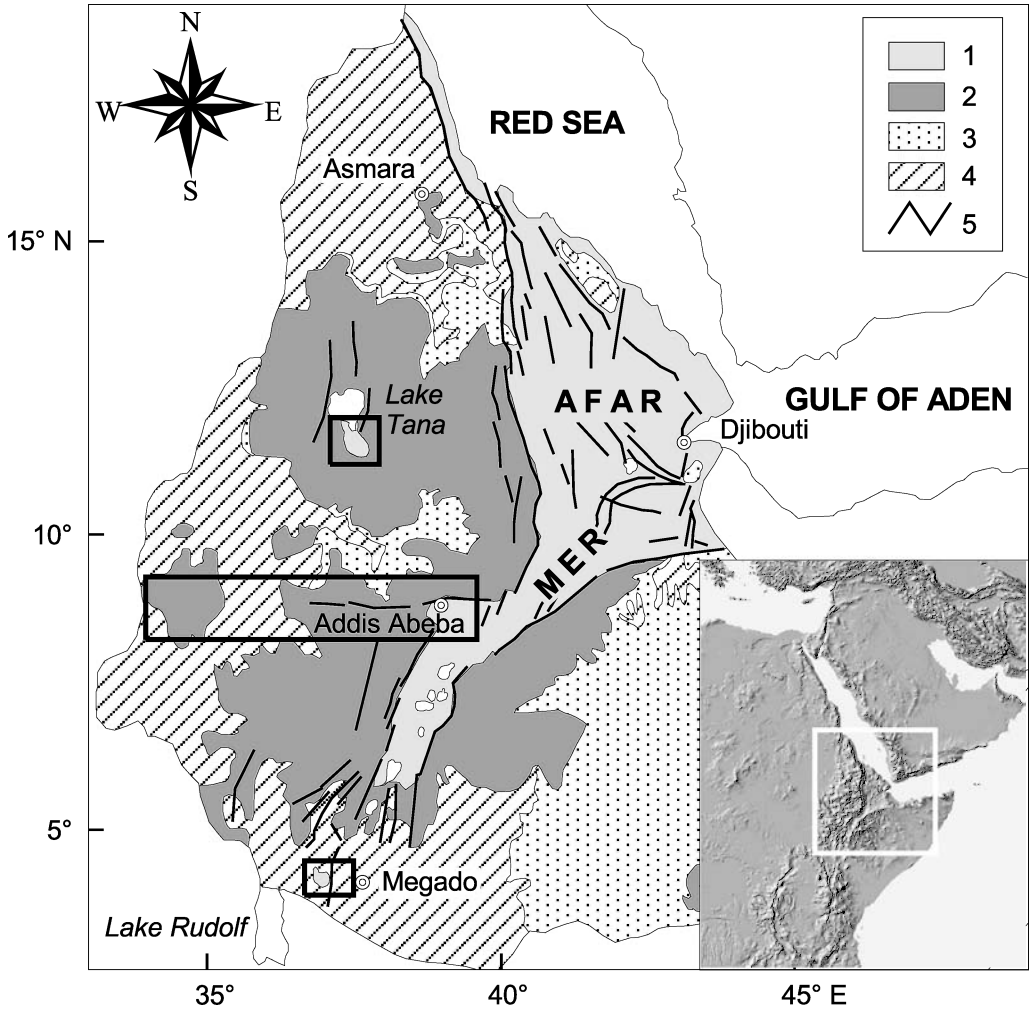

Fig. 1. Simplified geological map of the Main Ethiopian Rift (MER) and adjoning areas enclosed in the white rectangle of the shaded relief map reported in the inset. The black rectangles indicate the localities studied. *1* Late Miocene – Quaternary volcanic rocks; *2* Late Eocene – Early Miocene Ethiopian Volcanic Plateau; *3* Mesozoic continental and marine sedimentary rocks; *4* Proterozoic – Palaeozoic metamorphic basement; *5* major fault

the easternmost part of the YTVL) and in sectors far away from the MER (YTVL and Lake Tana).

The geographical distribution of mafic lavas along the YTVL offers also the opportunity for studying the lateral (∼500 km) continuity of subcontinental mantle domains. This paper is focussed on major and trace element data of petrographically fresh and relatively not evolved ($SiO_2 < 52$ wt.% and $MgO > 4$ wt.%) volcanic rocks, and is intended to provide a preliminary evaluation on the physico-chemical characteristics of the Ethiopian subcontinental mantle.

Geological background

The Afar triple junction (Fig. 1) offers the unique opportunity for studying the geodynamic evolution of a rift system, from the early stages of continental break-up to continental drift and sea floor spreading (e.g., *Kampunzu* and *Mohr*, 1991). Magmatism in the southern branch of the triple junction along the Kenyan and Ethiopian Rifts, the associated flood basalts and the volcanism of the Afar depression (collectively part of the EARS) represents one of the largest, currently active, continental igneous provinces (e.g., *Mohr* and *Zanettin*, 1988). Geochemical and geophysical evidence strongly points to the involvement of the Afar mantle plume in the generation of the Ethiopian flood basalts and the magmatism in Afar (*Schilling* et al., 1992; *Deniel* et al., 1994; *Scarsi* and *Craig*, 1996; *Hoffman* et al., 1997), and suggests that two periods of tectono-magmatic activity played a major role in shaping the region to its current form (e.g., *Courtillot*, 1982; *Mohr* and *Zanettin*, 1988; *Debayle* et al., 2001). A first period of uplift, rifting and magmatism has been identified in the Late Eocene – Early Miocene with the eruption of the voluminous Trap Series basalts in Yemen and Ethiopia, prior to the main rift apart of Arabia and Africa. A second period of uplift, rifting and magmatism began in the Late Miocene – Early Pliocene and has continued to the present with the development of the Main Ethiopian Rift and the nascent continental margins in the Red Sea and Gulf of Aden sea-floor spreading zones.

The Main Ethiopian Rift (MER), trending NNE–SSW, extends from ∼5° N to ∼10°50′ N where it widens into the Afar depression (Fig. 1), and was formed through the northward propagation of the Kenya Rift starting at ∼20 Ma and the southward migration of the SW branch of the Afar triple junction since the Late Miocene. The Rift Valley is bounded to the west by the Ethiopian Plateau, to the east by the Somalian Plateau, and is characterised tectonically by clusters of subparallel, NNE trending *en echelon* faults and eruptive fissures (e.g., *Baker* et al., 1972). The development of the MER was accompanied by an extensive bimodal volcanic activity that occurred both inside the rift and along its shoulders (e.g., *Gasparon* et al., 1993).

The Axum-Adua, Yerer-Tullu Wellel, and Goba-Bonga lineaments (*Abbate* and *Sagri*, 1980; *Mohr*, 1987; *Beyth*, 1991; *Abebe* et al., 1998) are important E–W regional structures, transversal to the MER axis, that dissect the rift. The Yerer-Tullu Wellel Volcano-Tectonic Lineament (YTVL), in particular, divides the Northern from the Southern Ethiopian Plateau, and represents an important lithospheric transtensional zone (*Abebe* et al., 1998). The lineament starts in the western margin of the MER, and extends westward up to the Sudan border. It is ∼500 km long and ∼80 km wide, and is marked by the occurrence of flood basalts and

several central volcanoes that are coeval with the volcanic activity of the MER. The YTVL is partly limited to the north by the Ambo fault which strikes E–W for some 150 km at ~9° N. Since the Late Miocene, the YTVL served as an important transtensional E–W structure having dominantly oblique, right lateral kinematics, probably acting along an inherited E–W trending structure (*Beyth*, 1991).

Three main lithostratigraphical successions outcrop along the YTVL: Proterozoic-Palaeozoic basement, Mesozoic continental and marine sedimentary rocks, and Cenozoic volcanics (*Abebe* et al., 1998 and references therein). Volcanic rocks are predominant, whereas the crystalline basement and sedimentary rocks are locally exposed by erosional processes and faulting. Two sequences have been recognised in the volcanic succession. The lower volcanic sequence, exposed mainly in the western and central areas, consists of flood basalts with associated trachytic and phonolitic domes and necks. It is strongly eroded and dissected by faulting, and locally unconformably covered by the products of the upper volcanic sequence. The lower volcanic sequence belongs to the uplifted Ethiopian Volcanic Plateau and is Oligocene to Early Miocene in age (*Abebe* et al., 1998). The upper volcanic sequence, which is Late Miocene to Quaternary in age, consists of several central volcanoes with associated small domes and cones, and minor fissure lava flows, all of which are roughly aligned E–W (Fig. 9a). The age distribution of the products of the upper volcanic sequence demonstrates that the volcanic activity started at ~10 Ma and developed in three main phases (*Miller* and *Mohr*, 1966; *Morton* et al., 1979; *Berhe* et al., 1987; *Wolde Gabriel* et al., 1990, *Abebe* et al., 1998). Fissure lava flows (e.g., the Anchar and Guraghe basalts, the basal lava flows of the Tullu Wellel Massif) erupted mainly during the oldest phase (10–7 Ma), whilst central volcanoes were formed during the second (6–2 Ma) and third (< 1 Ma) phase, with a roughly eastward migration of the foci of volcanism (Fig. 9a).

The other two sectors (Fig. 1) that have been studied in the present paper refer to the Pliocene – Quaternary volcanic activity recorded (i) in the southern part of the Lake Tana graben, some 350 km NW of Addis Abeba, and (ii) at Megado in the Sidamo region, the southermost part of the MER, close to the Kenyan border. These two localities are characterised by the occurrence of alkaline lava flow fields and monogenetic volcanic cones covering either the metamorphic basement or the Late Eocene-Miocene flood basalts (*Merla* et al., 1979; *Conticelli* et al., 1999).

Petrographical and geochemical outlines

During a reconnaissance field work (*Abebe*, 1995), more than 250 volcanic rock samples have been collected all along the Yerer-Tullu Wellel Volcano-Tectonic Lineament to maximise the variability in the traverse, and during a successive field work the sampling (~50 samples) was extended also in the other two sectors of Ethiopia (Fig. 1). The whole set of volcanic rocks belongs to transitional and alkaline series, with compositions varying from basanites, basalts and trachybasalts, to trachytes, peralkaline rhyolites and phonolites (*Abebe* et al., 1998; *Conticelli* et al., 1999). The YTVL samples are representative of both the Ethiopian Volcanic Plateau lavas and the Late Miocene – Quaternary volcanic rocks outcropping in the localities of, from east to west, Debre Zeyt, Wachacha, Guraghe, Wenchi, Rogghe Badda, Gibat, Ijaji, Konchi, Nekemt, Didessa, Tullu Wellel (Fig. 9a).

Table 1. *Average major (wt.%) and trace element (ppm) composition of the selected mafic lavas*

	EVP			Lake Tana			Megado			YTVL		
	avg 1σ	1σ %	n	avg 1σ	1σ %	n	avg 1σ	1σ %	n	avg 1σ	1σ %	n
SiO_2	49.52 ± 1.8	3.6%	(25)	47.01 ± 1.5	3.1%	(9)	43.90 ± 0.6	1.4%	(11)	47.44 ± 1.9	4.1%	(100)
TiO_2	2.32 ± 0.6	25.4%	(25)	1.67 ± 0.3	18.0%	(9)	2.40 ± 0.1	5.0%	(11)	2.21 ± 0.4	18.7%	(100)
Al_2O_3	16.35 ± 1.5	9.4%	(25)	17.24 ± 0.8	4.7%	(9)	14.10 ± 0.1	0.8%	(11)	17.11 ± 1.0	5.7%	(100)
Fe_2O_3	2.99 ± 1.6	54.4%	(25)	2.15 ± 1.3	62.2%	(9)	3.38 ± 0.3	9.7%	(11)	3.19 ± 2.0	61.7%	(100)
FeO	8.29 ± 1.9	22.9%	(25)	7.54 ± 0.9	11.4%	(9)	8.87 ± 0.4	4.8%	(11)	6.95 ± 1.8	25.5%	(100)
MnO	0.19 ± 0.0	13.6%	(25)	0.18 ± 0.0	15.4%	(9)	0.21 ± 0.0	9.6%	(11)	0.17 ± 0.0	10.2%	(100)
MgO	5.27 ± 0.8	16.0%	(25)	8.88 ± 1.2	13.1%	(9)	10.83 ± 1.2	11.1%	(11)	7.49 ± 1.9	25.5%	(100)
CaO	8.67 ± 0.9	10.9%	(25)	9.16 ± 0.4	4.7%	(9)	9.19 ± 0.2	1.6%	(11)	9.34 ± 0.9	10.2%	(100)
Na_2O	3.16 ± 0.3	10.0%	(25)	3.74 ± 0.6	15.5%	(9)	4.14 ± 0.4	9.2%	(11)	3.22 ± 0.5	15.3%	(100)
K_2O	0.96 ± 0.3	31.6%	(25)	1.41 ± 0.4	28.6%	(9)	1.74 ± 0.2	12.2%	(11)	1.22 ± 0.3	26.6%	(100)
P_2O_5	0.47 ± 0.2	43.6%	(25)	0.37 ± 0.1	18.9%	(9)	0.55 ± 0.0	6.8%	(11)	0.61 ± 0.2	36.4%	(100)
LOI	1.82 ± 0.7	39.1%	(25)	0.65 ± 0.2	37.2%	(9)	0.68 ± 0.1	16.7%	(11)	1.05 ± 0.6	58.2%	(100)
V	305 ± 51	16.6%	(25)	194 ± 25	12.8%	(9)	214 ± 26	12.1%	(11)	264 ± 47	17.9%	(100)
Cr	66 ± 44	67.0%	(25)	254 ± 108	42.8%	(9)	432 ± 58	13.4%	(11)	229 ± 164	71.7%	(100)
Co	43 ± 4	8.6%	(25)	41 ± 9	22.9%	(9)	44 ± 14	31.5%	(11)	47 ± 39	82.4%	(100)
Ni	35 ± 18	51.7%	(25)	165 ± 61	37.1%	(9)	309 ± 55	17.9%	(11)	114 ± 96	84.0%	(100)
Rb	19 ± 9	44.8%	(25)	46 ± 26	56.1%	(9)	44 ± 7	16.9%	(11)	26 ± 10	40.5%	(100)
Sr	440 ± 154	35.0%	(25)	616 ± 164	26.6%	(9)	798 ± 77	9.7%	(11)	679 ± 163	24.1%	(100)
Y	28 ± 7	26.7%	(25)	24 ± 4	15.9%	(9)	25 ± 3	13.6%	(11)	24 ± 7	28.6%	(100)
Zr	182 ± 49	27.1%	(25)	141 ± 30	20.9%	(9)	224 ± 35	15.5%	(11)	161 ± 53	33.2%	(100)
Nb	24 ± 9	38.5%	(25)	59 ± 32	54.1%	(9)	68 ± 11	16.1%	(11)	41 ± 15	36.7%	(100)
Ba	393 ± 161	41.0%	(25)	548 ± 231	42.1%	(9)	591 ± 71	12.1%	(11)	530 ± 129	24.4%	(100)
La	26 ± 11	43.9%	(25)	38 ± 20	51.4%	(9)	43 ± 8	17.7%	(11)	39 ± 16	40.3%	(100)
Ce	59 ± 18	29.9%	(25)	74 ± 34	45.5%	(9)	100 ± 16	16.0%	(11)	74 ± 25	33.0%	(100)

(*continued*)

Table 1 (*continued*)

	EVP			Lake Tana			Megado			YTVL		
	avg 1σ	1σ %	n	avg 1σ	1σ %	n	avg 1σ	1σ %	n	avg 1σ	1σ %	n
Al_2O_3/TiO_2	7.6 ± 2.5	32.3%	(25)	10.7 ± 2.1	19.8%	(9)	5.9 ± 0.3	4.9%	(11)	8.0 ± 1.6	20.1%	(100)
CaO/TiO_2	4.1 ± 1.4	34.9%	(25)	5.6 ± 0.9	16.8%	(9)	3.8 ± 0.2	3.9%	(11)	4.4 ± 0.9	20.2%	(100)
CaO/Al_2O_3	0.53 ± 0.04	7.1%	(25)	0.53 ± 0.05	9.0%	(9)	0.65 ± 0.01	1.7%	(11)	0.55 ± 0.07	12.9%	(100)
Zr/Nb	7.9 ± 1.9	24.0%	(25)	2.9 ± 1.1	39.0%	(9)	3.3 ± 0.1	3.8%	(11)	4.0 ± 0.9	22.7%	(100)
K/Nb	337 ± 61	18.2%	(25)	236 ± 81	34.4%	(9)	215 ± 9	4.0%	(11)	258 ± 56	21.8%	(100)
Rb/Nb	0.79 ± 0.21	26.2%	(25)	0.82 ± 0.25	30.4%	(9)	0.65 ± 0.05	7.3%	(11)	0.63 ± 0.17	26.6%	(100)
Ba/Nb	16.6 ± 6.0	36.3%	(25)	10.2 ± 2.1	20.7%	(9)	8.8 ± 0.6	6.4%	(11)	13.9 ± 4.6	33.4%	(100)
Ba/Rb	21.8 ± 8.0	36.7%	(25)	12.9 ± 2.49	19.4%	(9)	13.6 ± 0.86	6.3%	(11)	23.7 ± 10.7	45.1%	(100)
Ba/Ce	6.6 ± 1.7	25.9%	(25)	7.5 ± 0.9	11.6%	(9)	6.0 ± 0.7	12.2%	(11)	7.4 ± 1.6	21.6%	(100)

avg mean value; *1σ and 1σ %* standard deviation absolute and percentage; *n* number of samples analysed. The whole set of data is available as electronic supplementary material. *EVP* Oligocene – Early Miocene Ethiopian Volcanic Plateau mafic lavas along the YTVL; *YTVL* Late Miocene – Quaternary mafic lavas along the YTVL; *Lake Tana and Megado* Pliocene – Quaternary mafic lavas of the other two localities studied. Major elements have been determined by X-ray fluorescence spectrometry (XRF) with full matrix correction after *Franzini* et al. (1972), except MgO and Na_2O by atomic absorption spectrometry, and FeO by titration. Trace elements have been determined by XRF after *Kaye* (1965). Precision is <15% for V, Nb, Ba, <10% for Ni, Y, Zr, and <5% for other elements; accuracy has been tested on international standards and is <10%

The samples along the YTVL are characterised by a bimodal association. The mafic lavas generally have slightly porphyritic textures with variable phenocryst assemblages. In the area between the Debre Zeyt and Wenchi Volcano (Fig. 9a), the phenocryst assemblage is dominated by olivine + Ti-augite + plagioclase ± opaque minerals. In contrast the mafic rocks of the Gibat, Rogghe Badda and Nekemt Volcanoes are characterised by Ti-augite + olivine ± nepheline. Comendites, pantellerites and peralkaline trachytes occur mainly in the eastern sector of the YTVL, and are characterised by porphyritic textures with alkali feldspar + aegirine augite ± quartz ± aenigmatite ± alkaline amphibole ± opaques. Phonolites, tephriphonolites and nepheline-bearing trachytes are the evolved products of the central sector of the YTVL (Gibat, Rogghe Badda and Nekemt) and contain dominantly alkali feldspars (mainly anorthoclase) + nepheline + aegirine + alkaline amphibole ± opaques ± aenigmatite ± apatite. The rocks of the westernmost sector of the YTVL (Tullu Wellel, Fig. 9a) consist of a mildly alkaline to transitional association. The samples from the Lake Tana and Megado are restricted to mafic lavas and have aphyric to slightly porphyritic textures with olivine phenocrysts set in a micro- to cryptocrystalline groundmass of olivine + clinopyroxene + plagioclase + biotite (only Megado) + opaques ± apatite.

In order to assess the mineralogical and geochemical characteristics of subcontinental mantle domains, the whole set of samples has been carefully screened. First, the samples have been chosen to be essentially unaltered, with absence of secondary carbonates or zeolites. Second, only the less evolved samples ($SiO_2 < 52$ wt.%, $MgO > 4$ wt.%) have been selected, in order to minimise the effects of crystal fractionation on the chemical composition of lavas. This approach, although minimising the effect of crystal fractionation on incompatible trace element ratios, it does not totally preclude them. The compositional spread that we shall report here, however, is independent of the degree of evolution, such that the trace element

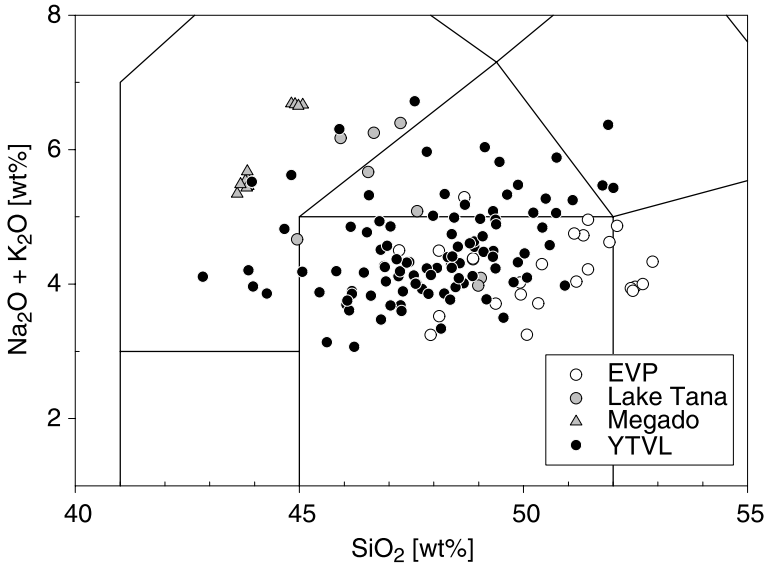

Fig. 2. Alkali *vs* silica (H_2O-free) classification diagram (*Le Maitre* et al., 1989) of the selected mafic lavas

characteristics of the eruptive rocks dominantly reflect mantle source composition and mantle processes.

Mean values and standard deviations of major and trace element composition of the different groups of the selected samples are reported in Table 1, and the whole set of data is available as electronic supplementary material. On the basis of alkali content (Fig. 2) and CIPW normative characteristics, the Late Miocene – Quaternary YTVL mafic lavas (hereafter YTVL) have a composition ranging from basanite to alkali basalt, hy-normative basalt, trachybasalt, and trachyandesite. The Ethiopian Volcanic Plateau lavas along the YTVL (hereafter EVP) have a composition ranging from hy-normative basalt and qz-normative basalt to basaltic andesite and hawaiite. The Lake Tana lavas have a compositional range similar to the YTVL samples although basanites prevail, whilst the Megado lavas are only basanites.

The subcontinental mantle reservoir

The major element content of the selected samples can provide a glimpse on the mineralogical characteristics of the subcontinental mantle reservoir. The Al_2O_3/TiO_2 and CaO/TiO_2 of basalts, in particular, vary systematically with the pressure and degree of melting, and the fertility of the source (e.g., *Fallon* and *Green*, 1988). In Fig. 3, the CaO/TiO_2 *vs* Al_2O_3/TiO_2 of the selected samples is compared with the evolved lavas of the YTVL (trachyte, phonolite, rhyolite) and the basalts of the Afar mantle plume. The selected samples are characterised by relatively low Al_2O_3/TiO_2 and CaO/TiO_2, similar to values displayed by the basalts of the Afar mantle plume and totally different from the evolved lavas of the YTVL. This

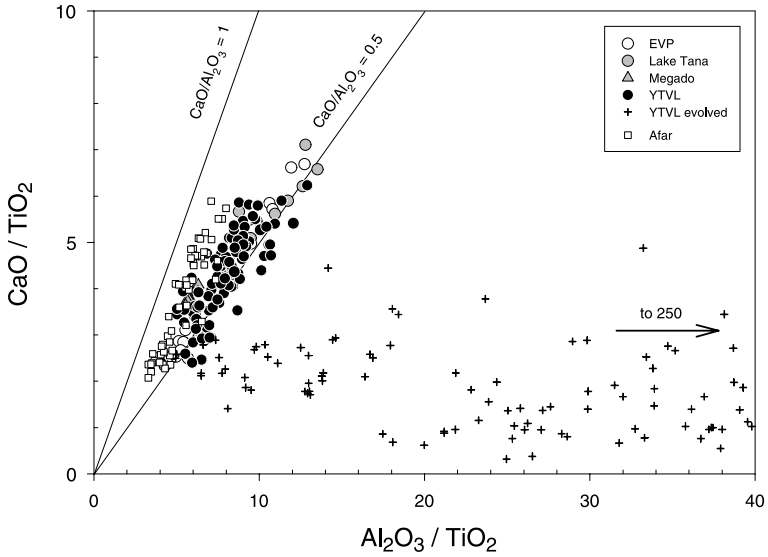

Fig. 3. CaO/TiO_2 *vs* Al_2O_3/TiO_2 diagram indicating the fertile *vs* refractory characteristics of the mantle source of the selected mafic lavas. The diagram includes also the basalts of the Afar mantle plume (*Deniel* et al., 1994) along with the evolved samples of the YTVL (*Abebe*, 1995) for comparison purposes. The straight lines with $CaO/Al_2O_3 = 1$ and 0.5 represent the compositional variation of mantle-derived magmas from oceanic areas (see the Petrological Database of the Ocean Floor at http://www.petdb.org/)

feature testifies to the reliability of the screened samples in terms of minimising geochemical variations due to low-pressure fractionation of mafic minerals, feldspar and Fe–Ti oxides. The samples have CaO/Al_2O_3 values ($0.55 \pm 13\%$, 1σ) falling on the low side of the range of mantle-derived magmas ($0.5 < CaO/Al_2O_3 < 1$, see caption of Fig. 3) and display no systematic increase of the ratio with increasing CaO/TiO_2 as slightly exhibited by basalts of the Afar mantle plume (Fig. 3). The constant CaO/Al_2O_3 along with the relatively low Al_2O_3/TiO_2 and CaO/TiO_2, provides evidence for a provenance from a relatively fertile mantle source at low degrees of melting (e.g., *Kushiro*, 1998).

A number of experimental petrology studies have been carried out to determine major element variations in basalts during mantle melting at different pressure (e.g., *Green* et al., 1979; *Jaques* and *Green*, 1980; *Stolper*, 1980; *Elthon* and *Scarfe*, 1984; *Takahashi*, 1986; *Fallon* and *Green*, 1988; *Hirose* and *Kushiro*, 1993; *Kushiro*, 1998). Overall, these studies demonstrated that basalts have systematic differences in major element composition and degree of silica saturation as a function of the temperature and pressure of mantle melting. *Albarede* (1992) demonstrated, following a principal component analysis, that the chemical variability of primary melts originated from mantle melting can potentially be used to construct empirical relationships relating SiO_2 and MgO content of basalts with the temperature and pressure of melt segregation from their mantle source. The drawback of this statistical analysis is that mineral fractionation during magma ascent is not taken into account and can represent a potential uncertainty.

The Mg-value [$\text{mol}\,100 \cdot MgO/(MgO + FeO)$] of the samples selected in our study (Fig. 4), along with Ni and Cr content (Table 1) clearly indicates that they are

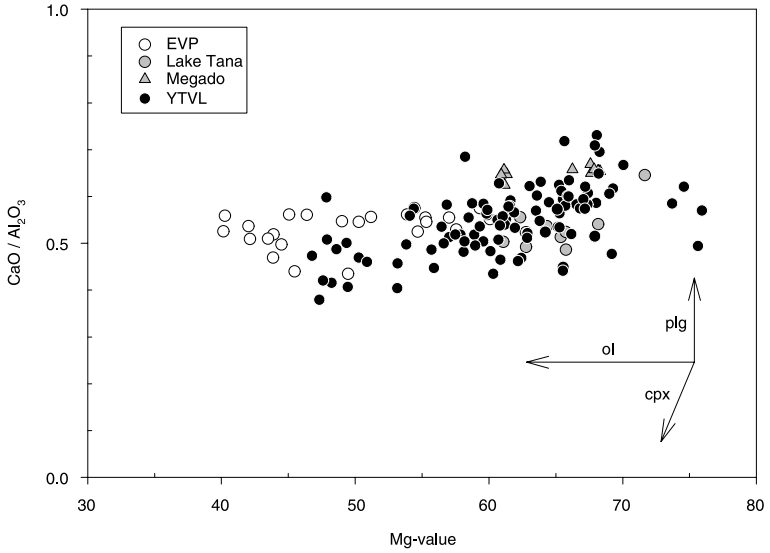

Fig. 4. CaO/Al_2O_3 *vs* Mg-value diagram of the selected mafic lavas indicating non-primary melt composition. The lines in the bottom right corner represent the evolution of liquids following olivine (ol), clinopyroxene (cpx) and plagioclase (plg) fractionation. The samples clearly indicate an olivine controlled liquid line of descent with negligible contribution of clinopyroxene. Mg-value: $\text{mol}\,100 \cdot MgO/(MgO + FeO)$, where FeO is 85% of FeO_{tot}

not primary melts (e.g., *Wilson*, 2000). The relatively constant CaO/Al_2O_3 ($0.55 \pm 13\%$, 1σ, Fig. 4), however, demonstrates that neither clinopyroxene nor plagioclase have fractionated extensively. This fact, coupled with the arguments presented by *Albarede* (1992) on the negligible effects on thermobarometric estimates of as much as 20% clinopyroxene and 25% plagioclase fractionation, give us confidence to calculate the primary magma composition considering only olivine fractionation. Using the method developed by *Pearce* (1978), and applying a K_D value of 0.3 between Fe^{2+}/Mg of olivine and melt (*Roeder* and *Emslie*, 1970), we have progressively added olivine to our samples until they were in equilibrium with typical upper mantle olivine composition ($\sim Fo_{90}$, e.g., *Wilson*, 2000). In most samples, the amount of olivine added has been in the range of 10–15 wt% (Lake Tana 11 ± 3, Megado 13 ± 4, YTVL 16 ± 6, 1σ), except the EVP samples (27 ± 7, 1σ), which have a more evolved composition (Fig. 4).

Once the primary magma compositions have been calculated, we have applied the empirical relationship given by *Albarede* (1992) to estimate the pressure of magma segregation from the mantle. We acknowledge that this method can have a large potential uncertainty because of the assumption made to estimate primary magma composition along with the common view that mantle melting is a polybaric process (e.g., *Langmuir* et al., 1992). Nonetheless, the results presented in Fig. 5 permit a number of qualitative considerations.

The pressure of melt segregation from the mantle appears to be confined within the lithospheric mantle (Fig. 5a), and all of the samples originated at similar depths (YTVL $= 2.1 \pm 0.6$ GPa, EVP $= 2.1 \pm 0.6$ GPa, Lake Tana $= 2.0 \pm 0.4$ GPa), but the Megado lavas (3.5 ± 0.1 GPa). Despite the similar depth of melt segregation, the EVP samples have higher Zr/Nb values (Fig. 5a). Mantle heterogeneity could be advocated to explain the different Zr/Nb signature of EVP and YTVL samples, although it is at odds with the similar pressure of melt segregation and the complete overlap of outcropping localities, i.e. their provenance is from the same mantle region. On the other hand, if we calculate a fictitious pressure of ''melt segregation'' (P_f), using as input parameters the chemical analyses of samples not corrected for olivine fractionation, we obtain a smooth negative gradient with Zr/Nb (Fig. 5b), with values increasing as pressure decreases. This fact provides arguments for a depth-related process (e.g., assimilation and/or chromatographic mechanism) acting during magma ascent, which has been more intense during the plateau building stage (EVP samples) than during the second period of magmatism (YTVL samples). The reason of this difference could be related to the higher amount of magma emplaced during the plateau building stage than during the second period of magmatism, which determined a higher heat flux and hence a potential greater opportunity to interact with ambient mantle and/or crust during ascent.

The negative Zr/Nb gradient (Fig. 5b) points to values encountered in crustal materials (bulk crust Zr/Nb $\sim$10, *Taylor* and *McLennan*, 1985), hence a twofold explanation is proposed: (i) a crustal component (e.g., the EM II component, *Zindler* and *Hart*, 1986) is present in the uppermost portion of the subcontinental mantle (<2 GPa) and the high heat-flow during the plateau building stage favoured interaction between the percolating EVP lavas and ambient mantle during ascent (e.g., *Hofmann*, 1972; *Navon* and *Stolper*, 1987; *Nielson* and *Wilshire*,

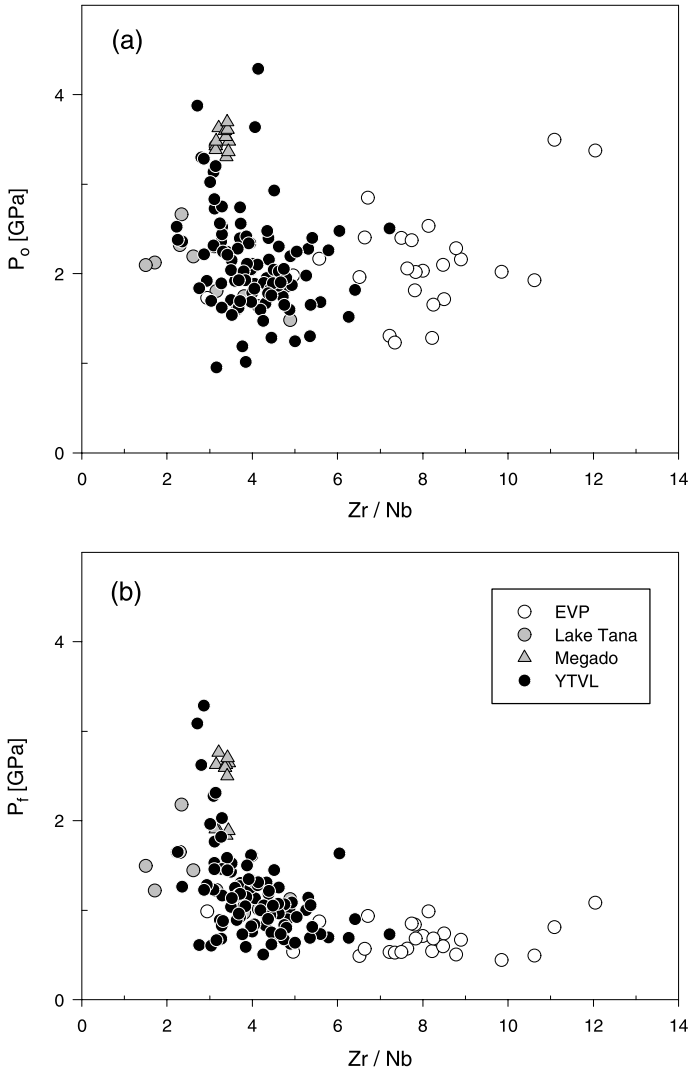

Fig. 5. **a** Estimated pressure (P_0) of melt segregation *vs* Zr/Nb indicating that the mantle source of the selected mafic lavas is within the lithosphere with average values of 2.1 ± 0.6 GPa (YTVL), 2.1 ± 0.6 GPa (EVP), 2.0 ± 0.4 GPa (Lake Tana), and 3.5 ± 0.1 GPa (Megado). **b** Fictitious pressure (P_f) of "mantle melting" *vs* Zr/Nb calculated using as input parameters the analyses of samples not corrected for olivine fractionation. The increase of Zr/Nb as P_f decreases could indicate a low pressure process *en route* to the surface (see text for explanation)

1993); (ii) the Zr/Nb signature of the EVP lavas is due to assimilation of crustal material during magma ponding at the base of the crust. Assimilation of crustal material, however, is expected to produce a correlation between trace element ratios and the degree of evolution (e.g., Mg-value), whilst the samples selected in our study do not exhibit any systematic covariation between Mg-value and, for example, Rb/Sr (Fig. 6), Ba/Rb, Rb/Nb, and Ba/Ce (not shown). Thus, the first explanation is more tenable and implies the presence of a vertically zoned subcontinental mantle underneath Ethiopia.

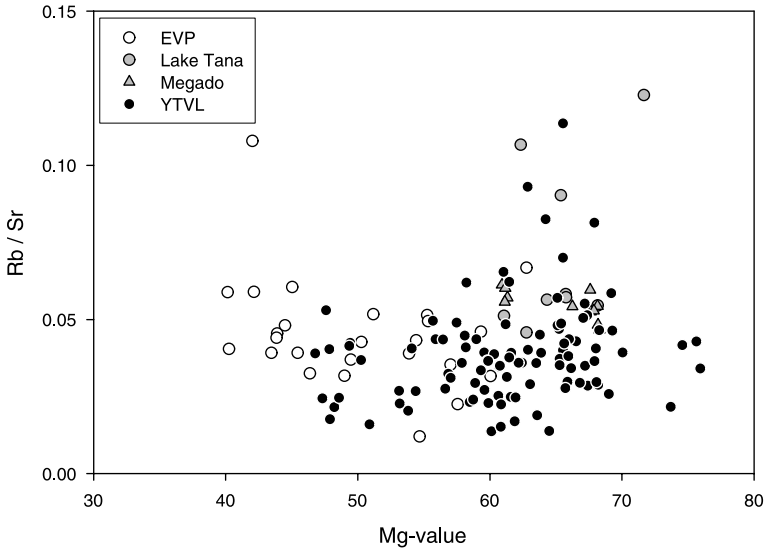

Fig. 6. Rb/Sr *vs* Mg-value diagram of the selected mafic lavas. Rb/Sr has no systematic variation with the degree of evolution as expected if the trace element signature of the EVP lavas were controlled by fractional crystallisation and assimilation (AFC) of crustal material (see text for explanation). Mg-value: mol $100 \cdot MgO/(MgO + FeO)$, where FeO is 85% of FeO_{tot}

Geochemical heterogeneity of the subcontinental mantle reservoir

The major element composition of the selected lavas demonstrate an origin from a fertile, subcontinental lithospheric mantle (~2–3.5 GPa), underneath the YTVL, Lake Tana, and Megado sectors. Additional information can be obtained combining major and trace element composition. For example, the CaO/TiO_2 *vs* TiO_2 diagram (Fig. 7a) is expected to exhibit a broad negative correlation because TiO_2 content is inversely correlated with the degree of melting whilst the opposite holds true for CaO/TiO_2 as long as clinopyroxene remains in the residue. Zr/Nb, however, exhibits correlation with neither CaO/TiO_2 (Fig. 7b) nor TiO_2 (not shown), i.e. the putative indicators of the degree of melting, despite the fact that Zr is slightly less incompatible than Nb during mantle melting (e.g., *Sun* and *McDonough*, 1989; *Hart* and *Dunn*, 1993). All of the samples but the EVP lavas have, in fact, a relatively constant and similar Zr/Nb (Table 1), indicating that (i) the ratio has not been significantly fractionated during melting, and (ii) the correlation between CaO/TiO_2 and TiO_2 may not be due to differences in the degree of melting (at least as the main process).

The first observation demonstrates that the Zr/Nb values of lavas are a source characteristic and indicate a relative homogeneity of the subcontinental mantle domains. This is also supported by the absence of correlation between CaO/TiO_2 and other trace element ratios that have different incompatibility during mantle melting, such as Rb/Y and Ce/Y (not shown). The lack of correlation of Zr/Nb with melting degree also in the EVP lavas (Fig. 7b), along with the negative gradient observed in Fig. 5b, reinforces the argument for different trace element enrichment factors in the uppermost mantle domains which modified the geochemical characteristics of the EVP lavas *en route* to the surface.

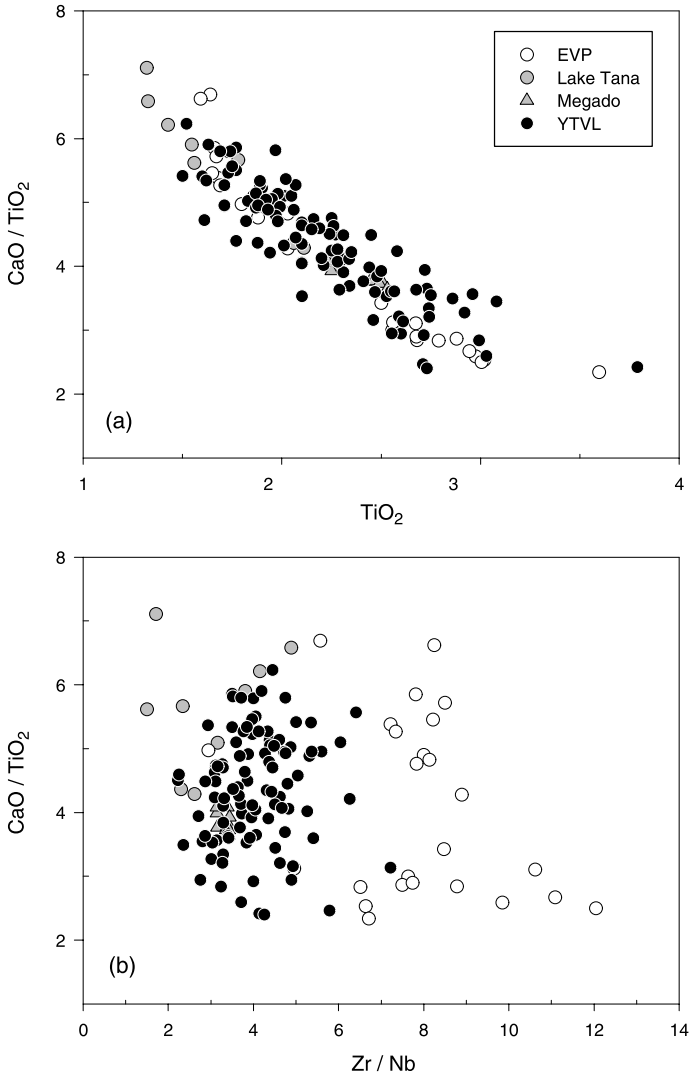

Fig. 7. CaO/TiO_2 *vs* TiO_2 (**a**) and Zr/Nb (**b**) diagrams of the selected mafic lavas. The inverse correlation between CaO/TiO_2 and TiO_2 could be consistent with different degrees of melting and the presence of clinopyroxene in the residue. However, the absence of correlation between CaO/TiO_2 and Zr/Nb, despite Nb is more incompatible than Zr during mantle melting, arises doubts on the fact that the correlation between CaO/TiO_2 and TiO_2 is caused by differences in the degree of melting (see text for explanation)

The second observation suggests that the cause of the correlation in Fig. 7a, could be due to differences in the fertility of the source and in different modal abundances of phases and/or components present in the source volume sampled during melting. For example, the relatively high CaO/TiO_2 of the Lake Tana samples (Fig. 7a) is coupled with high Al_2O_3/TiO_2 as well (Fig. 3), and indicates a slightly less fertile mantle source than the other samples. Moreover, the relatively constant Zr/Nb of all samples but the EVP lavas is at odds with the more than 6-fold variation in, for example, Ba/Rb (Fig. 8). In contrast to Zr and Nb (see

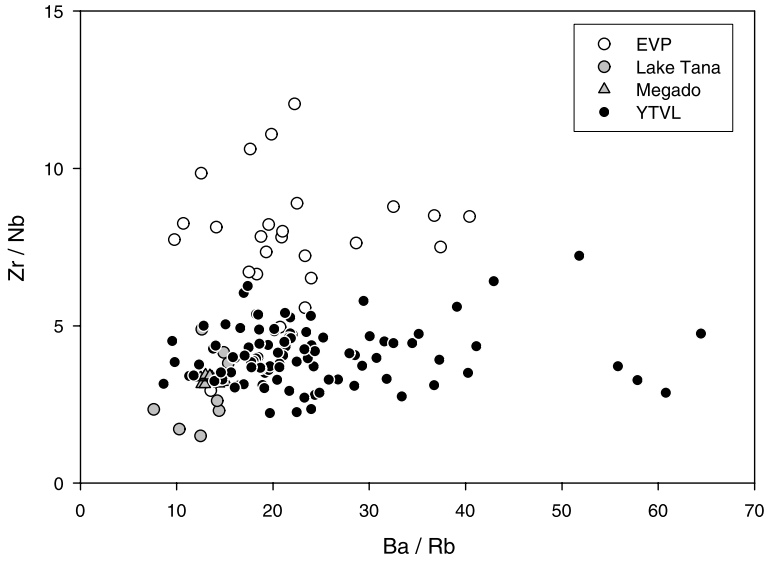

Fig. 8. Zr/Nb *vs* Ba/Rb diagram of the selected mafic lavas. The constant Zr/Nb of all of the samples but the EVP lavas is at odds with the more than 6-fold variation in Ba/Rb and demands for other processes than differences in the degree of melting to account for this variability

above), Rb and Ba have similar bulk distribution coefficients during mantle melting (e.g., *Sun* and *McDonough*, 1989); hence it is unclear why differences in the degree of melting can fractionate Ba/Rb but have no effect on Zr/Nb. As a corollary, it is more likely that the major and trace element signature of the selected samples is not correlated to the degree of melting but reflects the presence of different components in the mantle source.

In addition to these characteristics, the geographical distribution of the selected samples along the YTVL (∼500 km) can reveal important details on the lateral continuity of the subcontinental mantle reservoir. As already outlined in the geological background, the age of the Late Miocene – Quaternary magmatism along the YTVL progressively decreases towards the Main Ethiopian Rift (MER), and the youngest products (Fig. 9a) are coeval with the volcanic activity at Lake Tana and Megado. The estimated depth of melt segregation and the Zr/Nb value as a function of the distance from the MER has been reported in Fig. 9b and c. We have plotted also the Lake Tana and Megado samples for comparison.

The YTVL lavas, although scattered, display a general increase of the depth of melt extraction away from the MER (Fig. 9b), consistent with the geodynamic evolution of a rift zone. The Lake Tana lavas, despite being displaced some 350 km north of the YTVL, have a depth of melt extraction similar to the YTVL samples at the same longitude, whilst the Megado lavas have been originated in the deepest mantle levels (Fig. 9b). The Zr/Nb value (Fig. 9c) remains relatively constant all along the YTVL (except the EVP lavas) and the Lake Tana and Megado sectors. Overall, the subcontinental mantle reservoir sampled by the YTVL, Lake Tana, and Megado lavas (∼2.0–3.5 GPa) has a relatively homogeneous, fertile, and

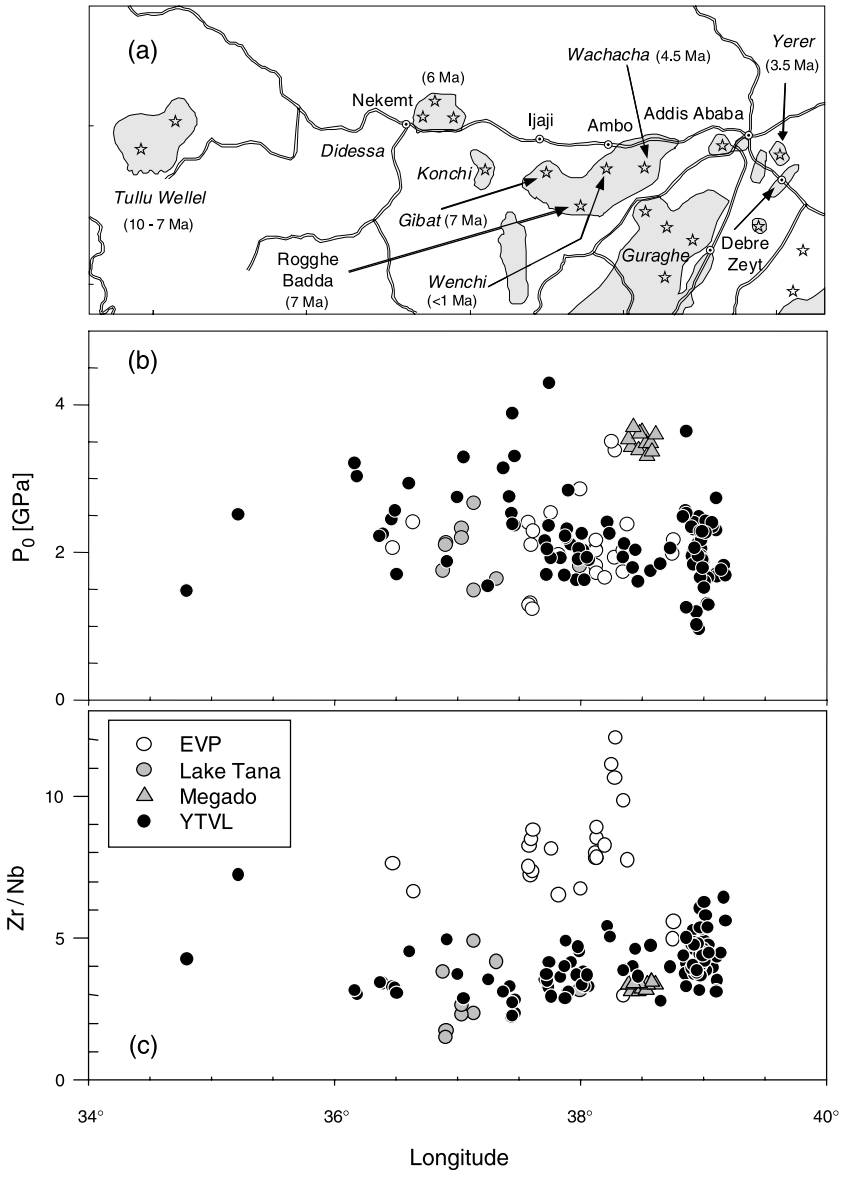

Fig. 9. Geochemical characteristics of the selected mafic lavas along the longitudinal extent of the Yerer-Tullu Wellel Volcano-Tectonic Lineament. The Lake Tana and Megado samples are reported for comparison. **a** Distribution of the main Late Miocene – Quaternary volcanic centres (gray areas) along the YTVL with their relative age of magmatic activity (*Miller* and *Mohr*, 1966; *Morton* et al., 1979; *Berhe* et al., 1987; *Wolde Gabriel* et al., 1990; *Abebe* et al., 1998). The other two diagrams depict the variation in the depth of melt extraction (**b**) and Zr/Nb (**c**) along the volcano-tectonic lineament

trace element enriched composition, whilst the EVP lavas, although generated at similar depths (Fig. 5a), have been likely modified during their passage through the shallower domain of the subcontinental mantle, which has different trace element enrichment factors.

Inferences on mantle components

Deciphering the mantle components present in the reservoir underneath the YTVL, Lake Tana, and Megado sectors requires a careful assessment of both trace element ratios and radiogenic isotopes (Sr, Nd, Pb, He etc.). In this study, therefore, we can only make a preliminary evaluation on the basis of key trace element ratios observed in the selected samples along with the mean values of potential mantle components. Most of the conclusions can be drawn from the K/Nb and Ba/Nb *vs* Zr/Nb variations observed in the selected samples (Fig. 10). The diagram reveals that a depleted mantle component (DMM, *Zindler* and *Hart*, 1986), as that sampled by N-MORBs, is not required in our case. On the basis of the occurrence of a vertically zoned subcontinental mantle along with the similar depth of melt segregation of all of the samples (Fig. 5), the data in Fig. 10 are best explained by a mantle reservoir located at ~2.0–3.5 GPa, with geochemical characteristics (low K/Nb, Ba/Nb, and Zr/Nb) similar to the subcontinental lithospheric mantle (SCLM) of *McDonough* (1990). The magma produced by this reservoir modified their geochemical signature to variable extent *en route* to the surface, through interaction with the uppermost portion (<2 GPa) of the mantle (e.g., *Hofmann*, 1972; *Navon* and *Stolper*, 1987; *Nielson* and *Wilshire*, 1993), which consists mainly of an enriched mantle component with a geochemical signature similar to the continental crust (high K/Nb, Ba/Nb, and Zr/Nb, Fig. 10). This enriched mantle can be identified as the EM II-type component (*Zindler* and *Hart*, 1986), albeit its proper definition requires the Sr and Nd isotope composition of the samples. The trace element signature of continental crust, however, overlaps with that of samples from ocean islands (Samoa and Society) representative of the EM II component (Fig. 10), indicating that this enriched mantle component can be identified also on the basis of trace element characteristics.

In agreement with the conclusion drawn from Fig. 5, the YTVL, Lake Tana, and Megado samples did experience only minor interaction with ambient mantle during ascent, whilst the geochemical signature of the EVP samples has been significantly modified during ascent, and acquired the composition of the enriched component (EM II) prevalent in the uppermost portion of the mantle (Fig. 10).

In addition to the vertical zoning of the subcontinental mantle underneath Ethiopia, the selected samples reveal an enrichment in K/Nb and Ba/Nb (Fig. 10) that cannot be caused only by interaction between the subcontinental lithospheric mantle (SCLM) and the enriched mantle component (EM II), but requires a metasomatising agent, which introduced fluid-mobile elements in the mantle reservoir and stabilised a K-bearing phase. A number of arguments have been presented in favour of either amphibole or phlogopite as potential candidates of K-bearing minerals in subcontinental mantle domains (e.g., *Michael*, 1988; *Guo* and *Green*, 1990; *Hawkesworth* et al., 1990). Data on amphibole- and phlogopite-bearing peridotites from the literature (e.g., *Zanetti* et al., 1996; *Ionov* et al., 1997), indicate that phlogopite has high K/Nb (>3000) and Ba/Nb (>50), whilst amphibole has moderate K/Nb (200–400) and low Ba/Nb (<5). Thus, the enrichment in K/Nb and Ba/Nb observed in our samples (Fig. 10) is likely due to the occurrence of trace amounts of phlogopite in the mantle reservoir, which contributed to melt production.

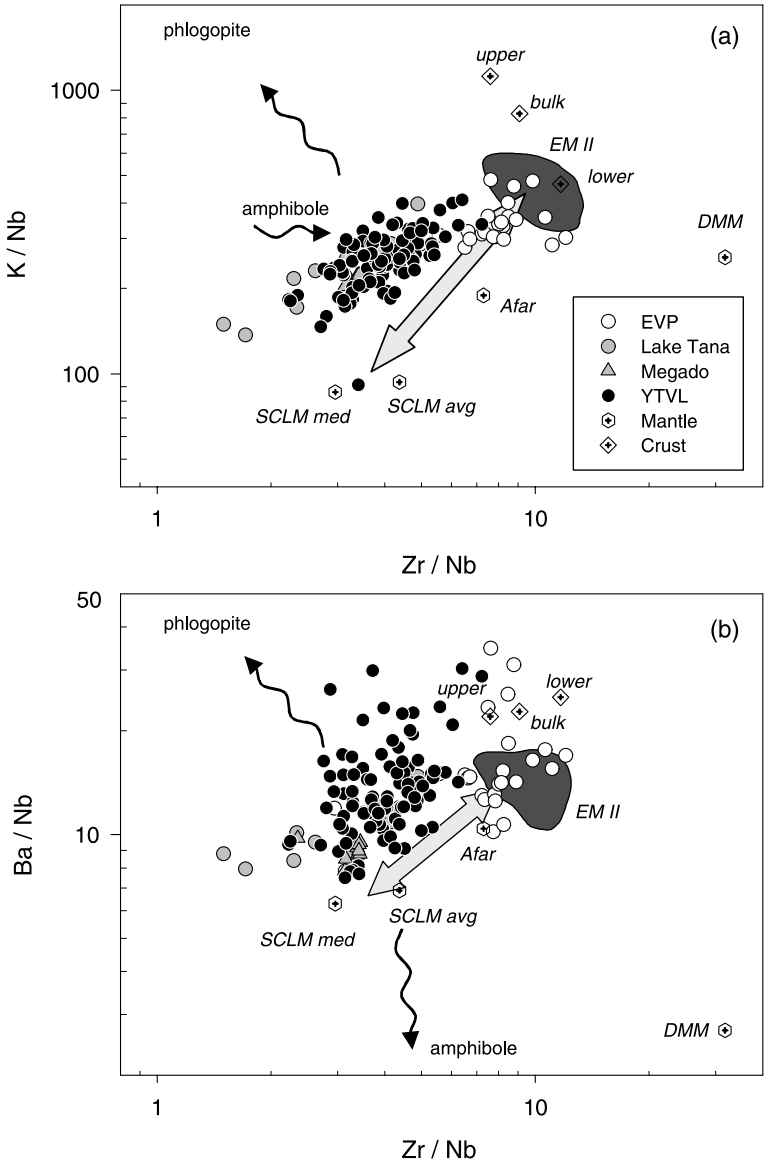

Fig. 10. K/Nb and Ba/Nb *vs* Zr/Nb diagrams assessing the mantle components in the subcontinental mantle domains underneath Ethiopia, sampled by the selected mafic lavas. The gray double arrow indicates a hypothetical interaction array between the subcontinental litospheric mantle (SCLM) and the enriched mantle component with a continental crust signature (EM II) (see text for discussion). The black arrows point to the amphibole and phlogopite composition in peridotites. Source of data – Mantle components: *DMM* average depleted mantle composition as sampled by N-MORBs (*Sun* and *McDonough*, 1989); *SCLM* subcontinental litospheric mantle, average (avg) and median (med) composition (*McDonough*, 1990); *Afar* average composition of lavas produced by the mantle plume underneath the Afar triple junction (*Deniel* et al., 1994); *EM II field* compositional range of mafic lavas from Samoa and Society islands with the highest $^{87}Sr/^{86}Sr$ (GeoRoc database at http://georoc.mpch-mainz.gwdg.de/georoc/). Crustal components: average composition of lower, upper and bulk crust (*Taylor* and *McLennan*, 1985). Amphibole and phlogopite compositions in peridotites are from *Zanetti* et al. (1996) and *Ionov* et al. (1997)

The presence of phlogopite in the source is also supported by the 6-fold variation in Ba/Rb of the selected samples (Fig. 8), which ranges from values typical of mantle-derived magmas (~11, *Sun* and *McDonough*, 1989) to values as high as 60. This is consistent with high Ba/Rb in phlogopite from mantle peridotites (e.g., *Zanetti* et al., 1996; *Ionov* et al., 1997) and reflects its non uniform distribution in the mantle reservoir. Upon melting, the random occurrence of trace amounts of phlogopite resulted in the observed "noise" to the main trend delineated by the samples (Fig. 10), between the subcontinental lithospheric mantle (SCLM) and the enriched mantle component (EM II), towards a scattered enrichment in Ba/Nb and K/Nb.

The presence of the Afar mantle plume is an additional end-member that can be neither disregarded nor confirmed with the available data, although its presence in the subcontinental mantle underneath the MER has been established on the basis of He isotopes (*Scarsi* and *Craig*, 1996). The same holds true for other OIB-related mantle components (e.g., HIMU, *Zindler* and *Hart*, 1986) whose assessment requires a detailed isotope systematics analysis, and it is beyond the scope of the present study.

Final remarks

The major and trace element composition of mafic lavas outcropping along the YTVL, Lake Tana and Megado sectors of Ethiopia, provides evidence for an origin by melting at ~2–3.5 GPa within a fertile and trace element enriched, subcontinental lithospheric mantle. The subcontinental lithospheric mantle is vertically zoned and has a relatively homogenous lateral continuity. The shallower domain (<2 GPa), as constrained on the basis of trace element characteristics of EVP lavas, has a different geochemical signature with respect to the deeper domain (~2–3.5 GPa) sampled by the YTVL, Lake Tana, and Megado lavas.

The preliminary scenario that can be inferred in these sectors of the East African Rift System is that of a deeper mantle reservoir with geochemical signature similar to the average subcontinental lithospheric mantle (SCLM, *McDonough*, 1990), and a shallower domain consisting of an enriched mantle component with a geochemical signature resembling crustal material and likely representing an EM II-type component (*Zindler* and *Hart*, 1986). Moreover, systematic enrichments in fluid-mobile elements provide evidence for a metasomatising agent that determined the formation of trace amounts of phlogopite in the mantle reservoir. The questions remaining to be answered refer to the timing of the processes that have modified the lithospheric mantle composition (Recent, Pan-African, Proterozoic) and the presence of other OIB-related end-members in the mantle reservoir.

Acknowledgements

This paper has benefited greatly from thorough reviews by *A. Heumann* and an anonymous reviewer. The research has been carried out with funds of the Italian CNR and MIUR, and part of the analytical work is from the Ph.D. thesis of *T.A.* We thank the Ethiopian Institute of Geological Survey for assistance during field work. We greatly appreciate the effort of people at the Lamont-Doherty Earth Observatory, USA, and at the MPI für Chemie, Mainz,

Germany, for making available the Petrological Database of the Ocean Floor and the GeoRoc database, respectively.

References

Abbate E, Sagri M (1980) Volcanites of Ethiopian and Somali Plateau and major tectonic lines. Atti Convegni Lincei 47: 219–227

Abebe T (1995) L'allineamento vulcano tettonico Yerer-Tullu Wellel (Etiopia centrale): evoluzione petrologica e vulcanologica di un sistema trasversale al rift Etiopico. Thesis, Università degli Studi di Firenze, 321 p

Abebe T, Mazzarini F, Innocenti F, Manetti P (1998) The Yerer – Tullu Wellel volcano-tectonic lineament: a transtensional structure in central Ethiopia and the associated magmatic activity. J Afr Earth Sci 26: 135–150

Albarede F (1992) How deep do common basaltic magmas form and differentiate? J Geophys Res 97 (B7): 10997–11009

Andersen T, O'Reilly SY, Griffin WL (1984) The trapped fluid phase in upper mantle xenoliths from Victoria, Australia: implications for mantle metasomatism. Contrib Mineral Petrol 88: 72–85

Arndt NT, Christensen U (1992) The role of lithospheric mantle in continental flood volcanism: thermal and geochemical constraints. J Geophys Res 97 (B7): 10967–10981

Baker BH, Mohr P, Williams RAJ (1972) Geology of the Eastern Rift System of Africa. Geol Soc Am Spec Papers 136: 67–78

Berhe SM, Desta B, Nicoletti M, Teferra M (1987) Geology, geochronology and geodynamic implication of the Cenozoic magmatic province in W and SE Ethiopia. J Geol Soc Lond 144: 213–226

Beyth M (1991) ''Smooth'' and ''rough'' propagation of spreading, southern Red Sea – Afar depression. J Afr Earth Sci 13: 157–171

Conticelli S, Sintoni MF, Abebe T, Mazzarini F, Manetti P (1999) Petrology and geochemistry of ultramafic xenoliths and host lavas from the Ethiopian Volcanic Province: an insight into the upper mantle under eastern Africa. Acta Vulcanol 11: 143–159

Courtillot V (1982) Propagating rift and continental break-up. Tectonics 1: 239–250

Debayle E, Léveque JJ, Cara M (2001) Seismic evidence for a deeply rooted low-velocity anomaly in the upper mantle beneath the northeastern Afro/Arabian continent. Earth Planet Sci Lett 193: 423–436

Deniel C, Vidal P, Coulon C, Vellutini PJ, Piguet P (1994) Temporal evolution of mantle sources during continental rifting: the volcanism of Djibouti (Afar). J Geophys Res 99 (B2): 2853–2869

Elthon D, Scarfe CM (1984) High-pressure phase equilibria of a high magnesia basalt and the genesis of primary oceanic basalts. Am Mineral 69: 1–15

Fallon TJ, Green DH (1988) Anhydrous partial melting of peridotite from 8 to 35 kb and the petrogenesis of MORB. J Petrol Spec Iss Lithosphere, pp 379–414

Franzini M, Leoni L, Saitta M (1972) A simple method to evaluate the matrix effect in X-ray fluorescence analyses. X-ray Spectrometry 1: 151–154

Gamble JA, McGibbon F, Kyle PR, Menzies MA, Kirsch I (1988) Metasomatised xenoliths from Foster Crater, Antartica: implications for lithospheric structure and processes beneath the Transantarctic Mountain Front. J Petrol Spec Iss Lithosphere, pp 109–138

Gasparon M, Innocenti F, Manetti P, Peccerillo A, Tsegayee A (1993) Genesis of the Pliocene to Recent bimodal mafic-felsic volcanism in the Dbre Zeyt area, central Ethiopia: volcanological and geochemical constraints. J Afr Earth Sci 17: 145–165

George R, Rogers N (1999) The petrogenesis of Plio-Pleistocene alkaline volcanic rocks from the Tosa Sucha region, Arba Minch, southern Main Ethiopian Rift. Acta Vulcanol 11: 121–130

Green DH, Hibberson WO, Jaques AL (1979) Petrogenesis of mid-ocean ridge basalts. In: *McElhinney MW* (ed) The Earth: its origin structure and evolution. Academic Press, London, pp 265–299

Guo J, Green TH (1990) Experimental study of barium partitioning between phlogopite and silicate liquid at upper mantle pressure and temperature. Lithos 24: 83–95

Hart SR, Dunn T (1993) Experimental cpx/melt partitioning of 24 trace elements. Contrib Mineral Petrol 113: 1–8

Hart WK, Wolde Gabriel G, Walter RC, Mertzman SA (1989) Basaltic volcanism in Ethiopia: constraints on continental rifting and mantle interactions. J Geophys Res 94 (B6): 7731–7748

Hawkesworth CJ, Rogers NW, van Calsteren PWC, Menzies MA (1984) Mantle enrichment processes. Nature 311: 331–335

Hawkesworth CJ, Kempton PD, Rogers NW, Ellam RM, van Calsteren PWC (1990) Continental mantle lithosphere and shallow level enrichment processes in the Earth's mantle. Earth Planet Sci Lett 96: 256–268

Hirose K, Kushiro I (1993) Partial melting of dry peridotites at high pressures: determination of compositions of melts segregated from peridotite using aggregates of diamond. Earth Planet Sci Lett 114: 477–489

Hofmann AW (1972) Chromatographic theory of infiltration metasomatism and its application to feldspar. Am J Sci 272: 69–90

Hofmann C, Courtillot V, Féraud G, Rochette P, Yirgu G, Ketefo E, Pik R (1997) Timing of the Ethiopian flood basalt event and implication for plume birth and global change. Nature 389: 838–841

Ionov DA, Griffin WL, O'Reilly SY (1997) Volatile-bearing minerals and lithophile trace elements in the upper mantle. Chem Geol 141: 153–184

Jagoutz E, Carlson RW, Lugmair G (1980) Equilibrated Nd – unequilibrated Sr isotopes in mantle xenoliths. Nature 286: 708–710

Jaques AL, Green DH (1980) Anhydrous melting of peridotite at 0–15 kbar pressure and the genesis of tholeiitic basalts. Contrib Mineral Petrol 73: 287–310

Kampunzu AB, Mohr P (1991) Magmatic evolution and petrogenesis in the East African Rift System. In: *Kampunzu AB, Lubala RT* (eds) Magmatism in extensional structural settings. Springer, Berlin Heidelberg New York, pp 85–136

Kaye MJ (1965) X-ray fluorescence determinations of several trace elements in some standard geochemical samples. Geochim Cosmochim Acta 29: 139–142

Kushiro I (1998) Compositions of partial melts formed in the mantle peridotites at high pressures and their relation to those of primitive MORB. Phys Earth Planet Int 107: 103–110

Langmuir CH, Klein EM, Plank T (1992) Petrological systematics of mid-ocean ridge basalts: constraints on melt generation beneath ocean ridges. In: *Morgan JP, Blackman DK, Sinton JM* (eds) Mantle flow and melt generation at mid-ocean ridges. Geophys Monogr, Am Geophys Union 71: 183–281

Le Maitre RW, Bateman P, Dudek A, Keller J, Lameyre J, Le Bas MJ, Sabine PA, Schimd R, Sorensen H, Streckeisen A, Woolley AR, Zanettin B (1989) A classification of igneous rocks and glossary of terms: recommendations of the International Union of Geological Sciences Subcommission on the systematics of igneous rocks. Blackwell, Oxford

McDonough WF (1990) Constraints on the composition of the continental lithospheric mantle. Earth Planet Sci Lett 101: 1–18

McKenzie D, Bickle MJ (1988) The volume and composition of melt generated by extension of the lithosphere. J Petrol 29: 625–679

Menzies MA, Kempton PD, Dungan M (1985) Interaction of continental lithosphere and asthenospheric melts below the Geronimo volcanic field Arizona, USA. J Petrol 26: 663–693

Menzies MA, Hawkesworth CJ (1987) Upper mantle processes and composition. In: *Nixon P* (ed) Mantle xenoliths. Wiley & Sons, London, pp 725–738

Menzies MA, Halliday AN (1988) Lithospheric mantle domains beneath the Archean and Proterozoic crust of Scotland. J Petrol Spec Iss Lithosphere, pp 275–302

Merla G, Abbate E, Canuti P, Sagri M, Tacconi P (1979) Geological map of Ethiopia and Somalia, 1:2,000,000 scale. National Council of Research (CNR), Roma, Italy

Michael PJ (1988) The concentration, behaviour and storage of H_2O in the sub-oceanic upper mantle: implications for mantle metasomatism. Geochim Cosmochim Acta 52: 555–566

Miller JA, Mohr PA (1966) Age of Wachacha trachyte-carbonatite centre. Bull Geophys Observatory Addis Ababa 11: 1–65

Mohr PA (1987) Patterns of faulting in the Ethiopian Rift Valley. Tectonophysics 143: 169–179

Mohr PA, Zanettin B (1988) The Ethiopian flood basalt province. In: *MacDougall JD* (ed) Continental flood basalt provinces. Kluwer, Dordrecht, pp 63–110

Morton WH, Rex DC, Mitchell JG, Mohr PA (1979) Riftward younging of volcanic units in the Addis Ababa region, Ethiopian rift valley. Nature 280: 284–288

Navon O, Stolper E (1987) Geochemical consequences of melt percolation: the upper mantle as a chromatographic column. J Geol 95: 285–307

Nielson JE, Wilshire HG (1993) Magma transport and metasomatism in the mantle: a critical review of current geochemical models. Am Mineral 78: 1117–1134

Pearce TH (1978) Olivine fractionation equations for basaltic and ultrabasic liquids. Nature 276: 771–774

Rogers N, Macdonald R, Fitton FG, George R, Smith M, Barreiro B (2000) Two mantle plumes beneath the East African rift system: Sr, Nd and Pb isotope evidence from Kenya Rift basalts. Earth Planet Sci Lett 176: 387–400

Roeder PL, Emslie RF (1970) Olivine-liquid equilibrium. Contrib Mineral Petrol 29: 275–289

Scarsi P, Craig H (1996) Helium isotope ratios in Ethiopian Rift basalts. Earth Planet Sci Lett 144: 505–516

Schilling JG, Kingsley RH (1992) Nd–Sr–Pb isotopic variations along the Gulf of Aden: evidence for Afar Mantle Plume – Continental Lithosphere interaction. J Geophys Res 97 (B7): 10927–10966

Stolper E (1980) A phase diagram for mid-ocean ridge basalts: preliminary results and implications for petrogenesis. Contrib Mineral Petrol 74: 3–27

Stolz AJ, Davies GR (1988) Chemical and isotopic evidence from spinel lherzolite xenoliths for episodic metasomatism of the upper mantle beneath southeast Australia. J Petrol Spec Iss Lithosphere, pp 303–330

Sun SS, McDonough WF (1989) Chemical and isotopic systematics of oceanic basalts: implication for mantle composition and processes. In: *Saunders AD, Norry MJ* (eds) Magmatism in the Ocean Basins. Geol Soc Lond Spec Publ 42: 313–345

Takahashi E (1986) Melting of dry peridotite KLB-1 up to 14 GPa: implicationson the origin of peridotitic upper mantle. J Geophys Res 91: 9367–9382

Taylor SR, McLennan SM (1985) The Continental Crust: its composition and evolution. Blackwell, Oxford

Waters FG, Erlank AJ (1988) Assessment of the vertical extent and distribution of mantle metasomatism below Kimberley, South Africa. J Petrol Spec Iss Lithosphere, pp 185–204

Wilson M (2000) Igneous petrogenesis. Kluwer, Dordrecht

Wolde Gabriel G, Aronson JL, Walter RC (1990) Geology, geochronology and rift basin development in the central sector of the Main Ethiopian Rift. Geol Soc Am Bull 102: 439–458

Zanetti A, Vannucci R, Bottazzi P, Oberti R, Ottolini L (1996) Infiltration metasomatism at Lherz as monitored by systematic ion-microprobe investigations close to a homblendite vein. Chem Geol 134: 113–133

Zindler A, Hart S (1986) Chemical geodynamics. Ann Rev Earth Planet Sci 14: 493–571

Authors' addresses: *S. Tommasini* (corresponding author; e-mail: toms@unifi.it), *P. Manetti* (e-mail: manetti@unifi.it), *T. Abebe* (e-mail: tsegu@geo.unifi.it), *M. F. Sintoni* (e-mail: sintoni@amnh.org), and *S. Conticelli* (e-mail: sandro.conticelli@geo.unifi.it), Dipartimento di Scienze della Terra, Università degli Studi di Firenze, Via La Pira 4, 50121 Firenze, Italy; *F. Innocenti* (e-mail: innocen@dst.unipi.it), Dipartimento di Scienze della Terra, Università degli Studi di Pisa, Via S. Maria 53, 50126 Pisa, Italy